INTEGRATED BIOINFORMATICS REVEALS POTENTIAL DRUG TARGETS IN HEPATOCELLULAR CARCINOMA

Hua Ngoc Minh Tuyen[1,*], Le Quan Hai[1], Phan Nguyen Hoang Khoi[1]

ABSTRACT

Introduction: Amongst the most prevalent cancers, hepatocellular carcinoma (HCC) is one of the cancers with high mortality rate due to limitation in diagnosis and treatment. In recent years, bioinformatics has become an effective tool, contributing significantly to the discovery and development of new drug**. Objective:** This study was carried out to evaluate prospective drug targets for the therapy of this illness by using bioinformatics tools. **Methods:** Microarray data from the dataset GSE147888, GSE101685, GSE62232 showing the gene expression in HCC patients was downloaded from the Gene Expression Omnibus. GEO2R was exploited to screen differentially expressed genes (DEGs) in HCC and normal counterparts. To identify possible drug targets, the protein-protein interaction network was investigated using Cytoscape, and the potential drug targets were validated using Gene Expression Profiling Interactive Analysis (GEPIA), Human Protein Atlas (HPA) and Kaplan-Meier plotter. **Results:** The study identified 538 DEGs comprising 227 up-regulated genes and 311 down-regulated genes. Among those genes, CDK1, CCNB1, CCNA2, CDC20, TOP2A, CCNB2 and MAD2L1 were confirmed as hub genes, which can serve as the important factors for the development of new targeted drugs. **Conclusion:** This study utilized an *in-silico* model to identify potential therapeutic targets for HCC, thereby highlighting the practical value of bioinformatics in discovering and developing novel treatment strategies for HCC.

Keywords: *Bioinformatics, drug target, HCC, liver cancer.*

I. INTRODUCTION

Hepatocellular carcinoma (HCC) is the most common and aggressive form of primary liver cancer, as reported by Globocan statistics [1]. Current treatment modalities—such as chemotherapy, radiotherapy, and surgical resection—are routinely employed; however, their therapeutic effectiveness remains limited, particularly in advanced stages of the disease. Consequently, the identification of novel drug targets for HCC has become an urgent priority to improve patient outcomes. In recent years, bioinformatics approaches have been increasingly utilized to analyze large-scale datasets across various diseases, including cancer, to uncover key genes, biomarkers, and molecular pathways involved in tumor initiation and progression [2, 3]. Several bioinformatics-based studies have identified genes associated with HCC. For instance, Yang et al. (2019) found several hub genes using integrated bioinformatics [4], while Regan-Fendt et al. (2020) found some novel genes and drugs against sorafenib resistant - HCC [5]. Nevertheless, due to the high degree of tumor heterogeneity in HCC, molecular characteristics can vary substantially among patients, highlighting the need to identify additional novel biomarkers that can support the development of more effective and personalized therapeutic strategies. Furthermore, drug repurposing offers a

[1] *Faculty of Pharmacy, Pham Ngoc Thach University of Medicine, Ho Chi Minh, Vietnam*
Responsible person: Hua Ngoc Minh Tuyen
Email: tuyenhnm@pnt.edu.vn
Date of receipt: 04/08/2025
Date of scientific judgment: 08/08/2025
Reviewed date: 08/09/2025

promising approach for accelerating the discovery of candidate compounds for cancer therapy, leveraging existing pharmacological agents for new clinical applications. Therefore, pinpointing potential therapeutic targets not only deepens the understanding of HCC pathogenesis but also provides critical guidance for the design of innovative treatment modalities.

In the present study, we systematically analyzed publicly available gene expression datasets using integrated bioinformatics tools to compare HCC samples with normal liver tissues. Our aim was to identify and evaluate differentially expressed genes (DEGs) with potential as druggable targets, thereby contributing to the development of targeted and personalized therapies for HCC.

II. METHODS

Data extraction from GEO database

Gene expression Omnibus (GEO; https://www.ncbi.nlm.nih.gov/geo/), was used to retrieve the public datasets. The datasets were selected based on the initial filter criteria using the keywords "hepatocellular carcinoma [All Fields] AND "Homo sapiens" [Organism] AND "expression profiling by array" [filter] AND "attribute name tissue" [Filter]", which resulted in the identification of 213 datasets. The datasets were then reviewed with the following description including: (a) Published from 01/01/2014 to 01/01/2025; (b) Involved in tumor samples derived from patients with HCC; (c) Includes both normal samples and HCC sample; (d) Comprise a minimum of 10 HCC samples and 5 healthy tissue samples as controls. After screening, we selected three datasets including GSE147888, GSE101685 and GSE62232, which consisted of 12 HCC and 12 control samples, 24 HCC and 8 control samples, 81 HCC and 10 control samples, respectively.

Detection of overlapping differential expressed genes

The data downloaded from GEO were analyzed using GEO2R tool (https://www.ncbi.nlm.nih.gov/geo/geo2r/) and Microsoft Excel to determine the differential expressed genes (DEGs) with the criteria of p-value < 0.05 and |logFC| (log – fold change) > 1 to obtain the corresponding DEGs of the 3 datasets. DEGs were next grouped based on logFC values, with logFC > 1 being up-regulated genes and logFC < -1 being down-regulated genes. The DEGs in each dataset were visualized using Volcano plot from GEO2R tool and the overlapping DEGs between all datasets were analysed with Venn diagram tool (https://bioinformatics.psb.ugent.be/webtools/Venn/).

PPI network generation and module analysis for hub gene identification

To identify key hub genes and core regulatory proteins involved in HCC, a protein–protein interaction (PPI) network was constructed using StringApp in Cytoscape software. Differentially expressed genes (DEGs) were input into the network, and an interaction confidence score threshold of > 0.7 was applied to ensure high-confidence interactions.

Subsequently, NetworkAnalyzer was used to assess topological parameters and identify hub nodes within the network. In parallel, Molecular Complex Detection (MCODE), a Cytoscape plugin, was employed to detect highly interconnected clusters or submodules within the PPI network. Modules were selected based on the criteria including "degree cutoff = 2, node score cutoff = 0.2, k-core = 2, and maximum depth = 100".

Hub gene validation with independent public databases

To validate the identified hub genes, several independent online platforms were utilized, including GEPIA (Gene Expression

Profiling Interactive Analysis), the Human Protein Atlas (HPA), and the Kaplan–Meier Plotter. The GEPIA platform was employed to check the expression levels of hub genes and to perform differential expression analysis between tumor and normal tissues using boxplot graph. The HPA database provided information on differences in protein expression between cancerous and normal tissues, thereby supporting the validation of transcriptional findings at the protein level through immunohistochemistry (IHC) data. In addition, the Kaplan–Meier Plotter tool (https://kmplot.com/analysis) was used to evaluate the prognostic significance of the hub genes, aiming to assess the correlation between gene expression levels and the overall survival of HCC patients.

III. RESULTS

Identification of overlapping DEGs

Differentially expressed genes (DEGs) were identified by comparing gene expressions in HCC tissue samples with corresponding normal liver tissue samples in each dataset. To minimize bias due to heterogeneity between datasets, normal control samples were not pooled from different datasets. Three microarray datasets, namely GSE147888, GSE101685, and GSE62232, were used in the analysis, consisting of a total of 117 HCC samples and 30 normal liver tissue samples. The DEGs were filtered based on statistical thresholds with a p-value < 0.05 and |logFC| > 1 (Figure 1A). Venn diagram analysis was performed to identify the overlapping DEGs across the datasets, resulting in a total of 539 common DEGs (Figure 1B). Notably, one gene appeared as both upregulated and downregulated in different datasets, which was possibly due to dataset variability. After accounting for this, 227 up-regulated genes and 311 down-regulated genes were listed in Table 1. These DEGs represent consistent expression changes across all three datasets.

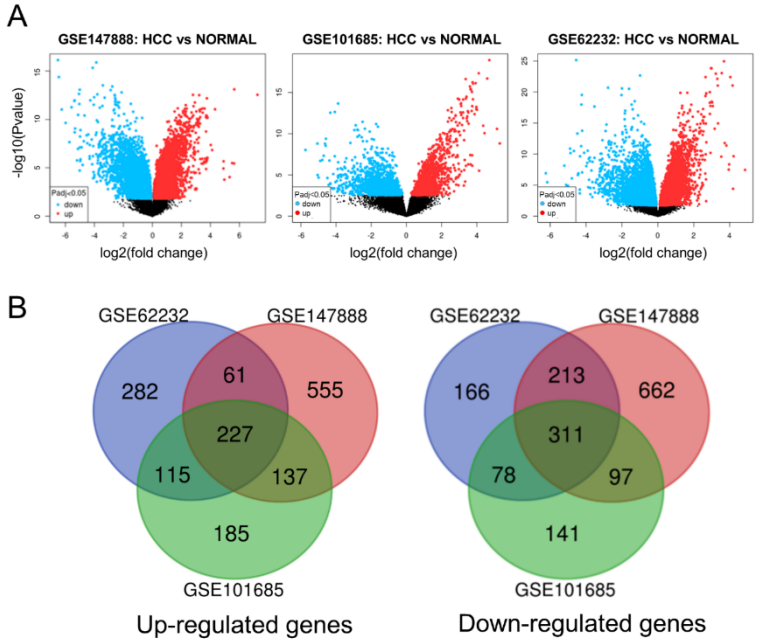

Figure 1. ***Visualization and analysis of DEGs.***

(A) Expression of DEGs in microarray dataset GSE147888, GSE101685 and GSE62232 were visualized by volcano plot. (B) A Venn diagram was constructed to visualize the overlapping DEGs between three datasets.

Table 1: ***List of overlapping differentially expressed genes***

Group	Gene names
Up-regulated genes	AACS; E2F8; C1orf106; SPINK1; TKT; HSPB1; DNAH14; TPX2; GPSM2; CENPQ; C15orf48; IGF2BP3; CCNB1; XK; IGSF3; FLVCR1; HOXA13; TTF2; CCDC34; AKR1B10; ZIC2; KPNA2; ANLN; ST8SIA6-AS1; BIRC5; WHSC1; MIS18A; KNTC1; FOXM1; COL15A1; EZH2; RBM24; CDK1; FABP5; KIF11; RACGAP1; C12orf75; CDC6; SULT1C2; KIF2A; CENPU; NEU1; SAC3D1; ENAH; SMC4; TDRKH; PLXNC1; AURKA; FOCAD; KIF14; MAD2L1; ATP6V1C1; ALYREF; NMRAL1P1; C1orf112; MCM3; TTC13; TUFT1; PDSS1; RHNO1; NEDD4L; GAS2L3; CENPL; KIF4A; CPD; OSBPL3; CAPG; CCL20; ROBO1; SPP1; MPZL1; BARD1; SPDL1; RAB11FIP4; KIF2C; SQLE; MCM10; TCF19; DNMT3A; ITGA6; EBF1; UBE2Q2; ACLY; TYMS; CDCA7; MCM5; TMEM106C; MELK; PODXL; CDC20; CDKN2B; HN1; ZWINT; NDC80; ITGA2; H2AFZ; RFC4; H2AFX; OIP5; CCNA2; GTSE1; BUB1; NUF2; PBK; COCH; TRIP13; LAMC1; CA12; NEB; PTTG1; HMGB2; MMP12; CDC7; STMN1; UBE2T; CRNDE; TRIM6; CD109; CKS2; TP53I3; TBC1D16; ECT2; DEPDC1; ANXA2; PRKAA2; EPPK1; IKBIP; COLCA2; MTFR2; CENPE; ASPM; UBE2S; CD24; CDCA3; PLCB1; SRXN1; LOXL2; ATAD2; KNL1; DNMT1; NQO1; STXBP6; MND1; CHML; CCNB2; RAB3B; TTC39A; TPGS2; POLE2; PRC1; SLC1A4; SMARCA4; CENPW; CKAP2; CEP55; RRM2; G6PD; MDK; TOP2A; FEN1; HELLS; FANCI; CCNE2; SSX1; TMEM38B; NCAPD2; ASNS; MCM2; TRIM71; MCM4; DCAF13; KIF15; MSH2; BUB1B; DLGAP5; RAD51AP1; LRRC1; CEP41; RNASEH2A; MKI67; CAP2; DTL; FAM83D; EFCAB2; SUCO; TOMM40L; LPL; HMMR; PKM; GPC3; CDKN2C; MCM6; GMNN; SOWAHA; DLG5; KIF20A; RRAGD; CENPK; SAE1; DSN1; RNF157; PLVAP; PEG10; WDYHV1; CTHRC1; UHRF1; BCAT1; CDKN2A; SGO2; KIAA0101; TTK; MCM8; CDKN3; NME1; NCAPG; FDPS; RMI2; LAPTM4B; NEK2; ACSL4; RCN2; TMEM206; CENPF; NUSAP1; FANCD2; PSPH; ESM1.
Down-regulated genes	PTN; CYP26A1; XDH; CXCL14; IGF1; CYP39A1; MBNL2; HMGCS2; EPB41L4B; FAM134B; PROZ; ZG16; SLC25A37; DEPDC7; LDHD; SYNPO2; RCL1; NR4A2; SLCO1B3; SORL1; FCGR2B; BCO2; ACSM3; CYP2C19; ACAT1; DACH1; FOLH1B; GHR; CLEC1B; STARD5; STEAP3; SHBG; ATOH8; SPRYD4; DNASE1L3; PPM1K; CPEB3; C8orf4; FAM198A; ID1; C1orf168; GPD1; CRHBP; IDO2; IGFALS; BDH2; ETS2; PTPRB; ACADL; PRRG4; DBH; TBXA2R; CBR4; MYO10; COLEC11; SRD5A2; ADRA1A; ECM1; AKR7A3; PBLD; MPC1; MS4A6A; CYP4V2; FCN2; KLKB1; F11; GNAO1; MT1G; FAM149A; CYP2A6; PLSCR4; PPARGC1A; CDC37L1; PGLYRP2; LINC01093; ALDH6A1; NDRG2; TMEM47; MFSD2A; NGFR; APOA5; FYN; HOGA1; CYP2B7P; ARHGEF26; CFHR4; PPP1R3B; ASPA; RCAN1; NTN4; EDNRB; DSE; MAN1C1; MYCT1; ST3GAL6; ALDH1B1; DUSP1; KBTBD11; CYP2C9; ACVR1C; GCGR; CYP2A7; KDM8; CTH; GRHPR; CLEC4M; GABARAPL1; NPY1R; ESR1; CYB5D2; CYP4F12; VSIG4; GCH1; NDFIP2; RND3; IL1RAP; RDH16; PER2; TMEM27; TPD52L1; CSRNP1; MME; LPAL2; CYP4A11; THRSP; ART4; ACAA2; C7; S100A8; ZFP1; FOXO1; AADAT; PDK4; GPM6A; NNMT; SLC9B2; MOGAT2; MAGI2-AS3; SAMD5; TLR3; CPED1; EPHX2; IVD; GCDH; APOF; ANGPTL1; FAM13A; GADD45B; MRO; ACSM5; GRAMD1C; FERMT2; TUBE1; GREM2; NR3C2; DIRAS3; CD163; SIGIRR; DPF3; SLC25A47; GAREM1; SKAP1; GADD45G; PDE2A; AXL; RORA; CDC14B; PRG4; CCR1; NAMPT; CYP1A2; UROC1; CCDC3; CDO1; ANXA10; TSKU; GYS2; ETFDH; LPA; CD5L; C8B; KLHL15; CXCL2; TAT; LIFR; EXPH5; COLEC10; LYVE1; CYP2C18; STAB1; SRD5A1; NAAA; FOS; P3H2; MUT; NAT2; MASP2; MMAA; AKR1D1; PAMR1; ENPEP; GNE; CXCL12; FEZ1; AVPR1A; EHD3; CSAD; DGAT2; ACSL1; SPATA18; CYP3A43; SYNE1; GCKR; GPR146; FBP1; ADH4; OIT3; GLYAT; ANGPTL6; CETP; HBB; SRPX; MAT1A; MSRA; MS4A7; MPDZ; ADAMTS13; HAND2-AS1; IYD; SOCS2; TSLP; TMEM220; RBMS3; HAO2; PLPP3; IL33; TGFBR3; HAAO; HHIP; ADH1B; PEMT; KCNN2; GSTZ1; EVA1A; LY6E; ITGA9; OLFML3; CNDP1; TKFC; CCDC71L; FAXDC2; FCN3; ACACB; GBA3; RNF125; ECHDC2; CLEC4G; CYP2B6; CCBE1; KMO; MASP1; MAP2K1; IRF8; ANK3; FOSB; FAM65C; CLRN3; CFHR3; MARCO; ADH6; LCAT; TDO2; VIPR1; RSPO3; IGFBP3; PLAC8; HAMP; DCN; CFP; S100A12; N4BP2L1; JDP2; FTCD; CIDEB; TFPI2; TIMD4; LHX2; STAB2; NAT1; DHODH; PTH1R; HGFAC; ADGRG7; CDA; ZGPAT; TMEM56; OGDHL; ADGRA3; KAZN; PZP; SFRP1; HGF; GGT5; CYP3A4; TPPP2; GPAT3; SATB1; C1QTNF1; PTGIS; BCKDHB; ANKRD37.

PPI network construction and analysis

The DEGs obtained from GSE147888, GSE101685, GSE62232 were imported into StringApp of Cytoscape for the analysis of the PPI with 528 nodes and 2099 edges (Figure 2A). Using Network Analyzer tool, the top 11 DEGs with the highest node degree score were shown (Figure 2B). Besides, the MCODE plugin has defined one of the most significant modules from the original PPI (Figure 2C). 46 genes were found to be involved in this module, including ECT2, DEPDC1, ZWINT, AURKA, CDC20, CENPE, PTTG1, CDKN3, MKI67, NUF2, PBK, KIF11, ANLN, TTK, BUB1B, DLGAP5, ASPM, NEK2, NCAPG, CENPF, NUSAP1, HMMR, NDC80, KIF15, CEP55, KIF2C, CCNB2, PCLAF, TOP2A, BUB1, BIRC5, CCNB1, KIF4A, RACGAP1, RRM2, CCNA2, CDK1, TPX2, CDCA3, PRC1, MAD2L1, KIF14, FOXM1, TRIP13, MELK, KIF20A. Supprisingly, those top 11 DEGs with highest node degree score were also included in the most significant module. Therefore, those 11 genes were considered as the initial hub genes, including CDK1, CCNB1, CCNA2, CDC20, TOP2A, BUB1B, KIF11, BUB1, CCNB2, MAD2L1, NUF2.

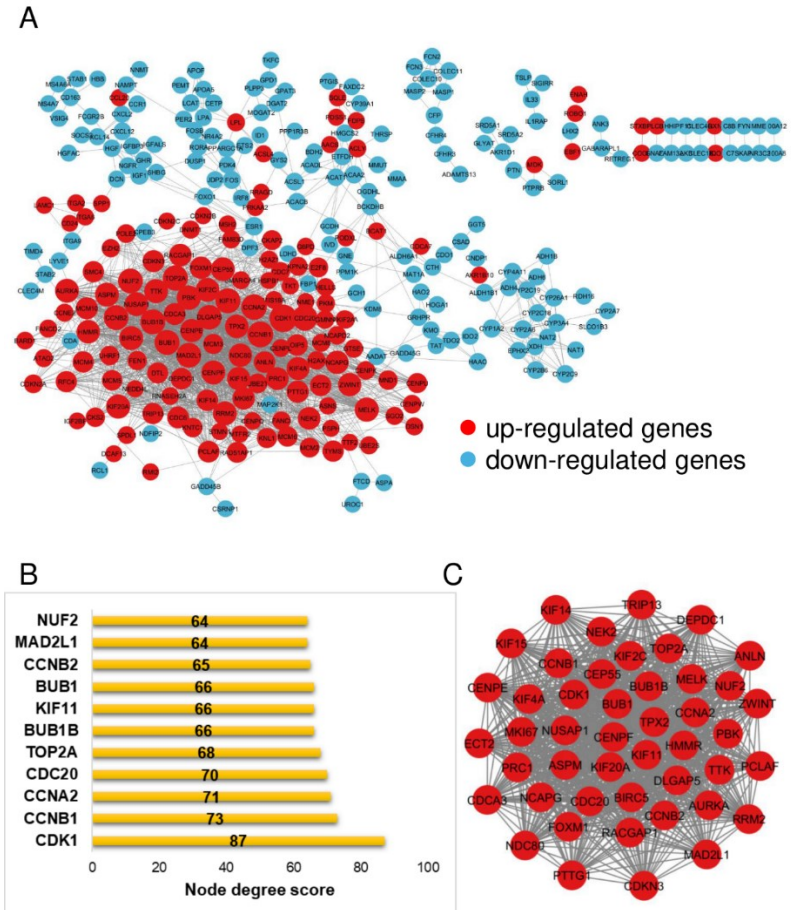

Figure 2. ***Visualization and analysis of protein-protein interaction (PPI) network.***
(A) PPI network. (B) The top 11 DEGs with high node degree score calculated by Network Analyzer. (C) The most significant module analysed by MCODE plugin.

Selecting and validating the hub genes

The initial hub genes were validated using GEPIA, HPA and Kaplan Meier-plotter. As the result, GEPIA showed that 10/11 initial hub genes including CDK1, CCNB1, CCNA2, CDC20, TOP2A, BUB1B, BUB1, CCNB2, MAD2L1, NUF2 were statistically experssed higher in tumor tissues compared to normal ones (Figure 3).

We next performed protein expression using HPA database with 10 genes after narrowing down with GEPIA. Among them, 7/10 genes including CDK1, CCNB1, CCNA2, CDC20, TOP2A, CCNB2, MAD2L1 (but not BUB1, BUB1B and NUF2) exhibited significant differences between HCC and normal tissues at the protein level based on the immunohistochemistry staining in HPA (Figure 4).

Since the expression of potential drug target should reflect the prognosis of liver cancer, we exploited Kaplan Meier plotter to identify the link between gene expression and patient overall survival. The analysis showed that 7/7 hub genes after validating with GEPIA and HPA expressed the inverse correlation between gene expression and survival time, meaning that high expression of those genes linked to shorter survival in liver cancer patients. Therefore, 7 hub genes including CDK1, CCNB1, CCNA2, CDC20, TOP2A, CCNB2 and MAD2L1 have been identified as potential drug targets (Figure 5).

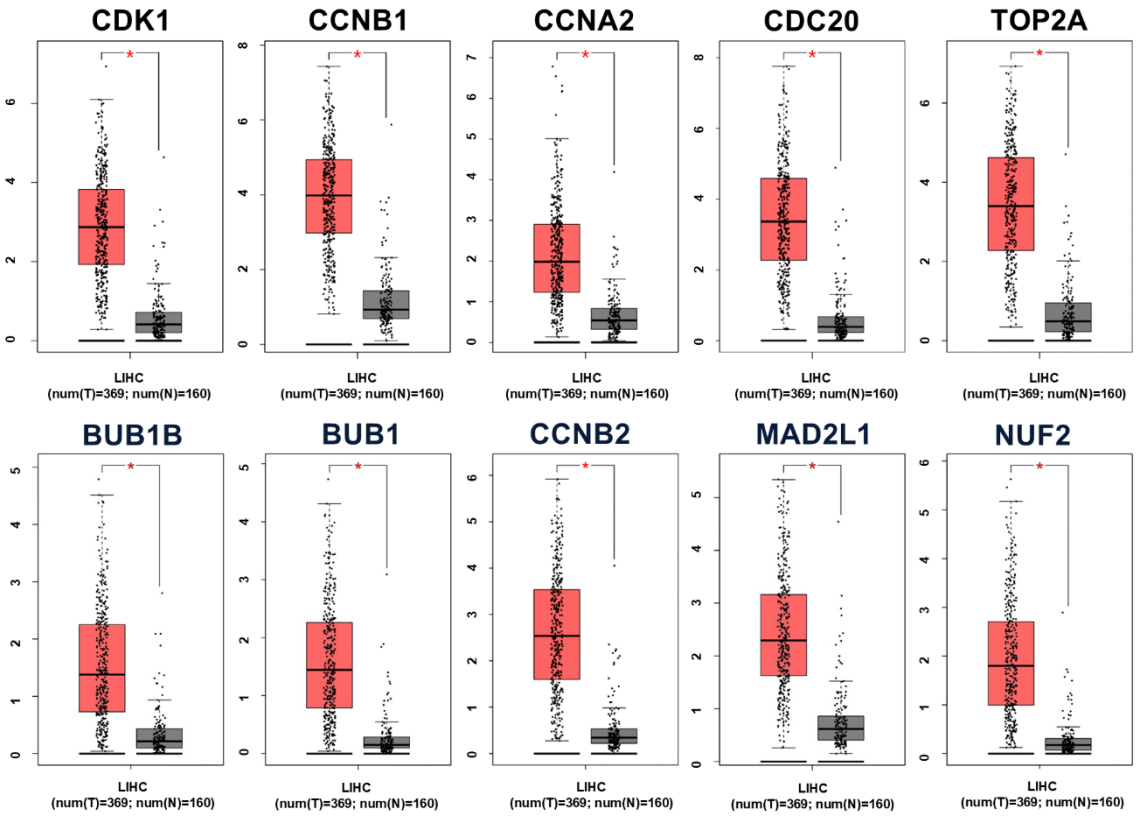

Figure 3. ***The gene experession of the hub genes in tumor tissues compared to normal ones in GEPIA database.*** * Indicates *p*-value < 0.05.

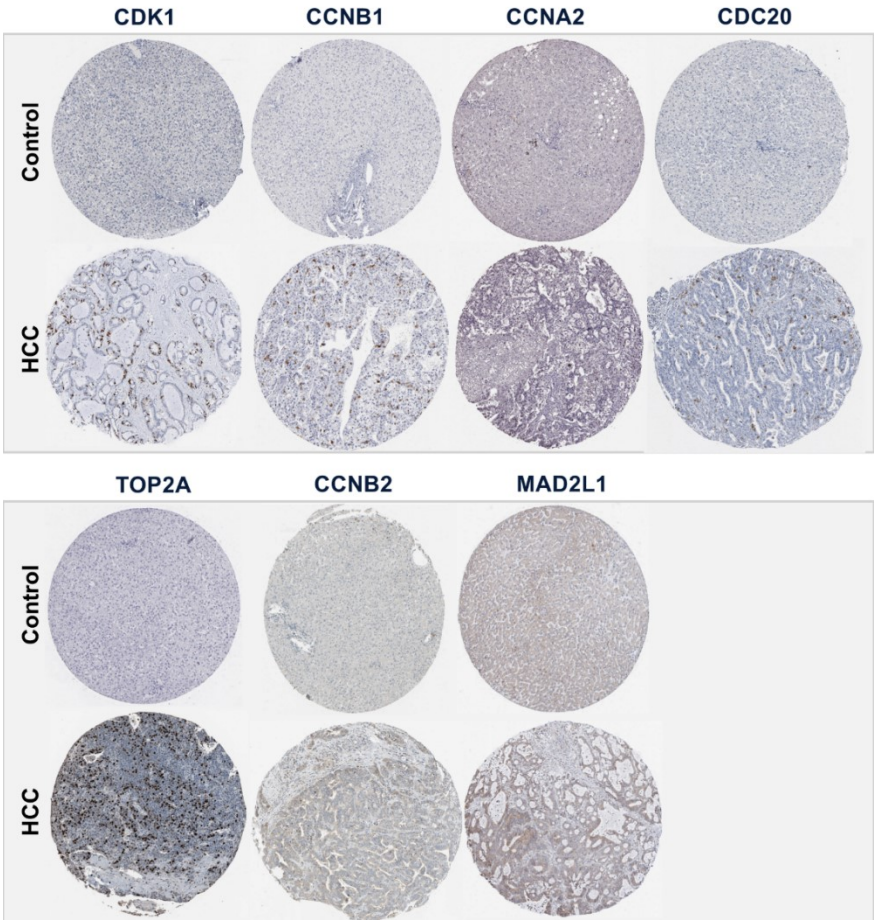

Figure 4. ***The protein experession of the hub genes in tumor tissues compared to normal ones in HPA database.***

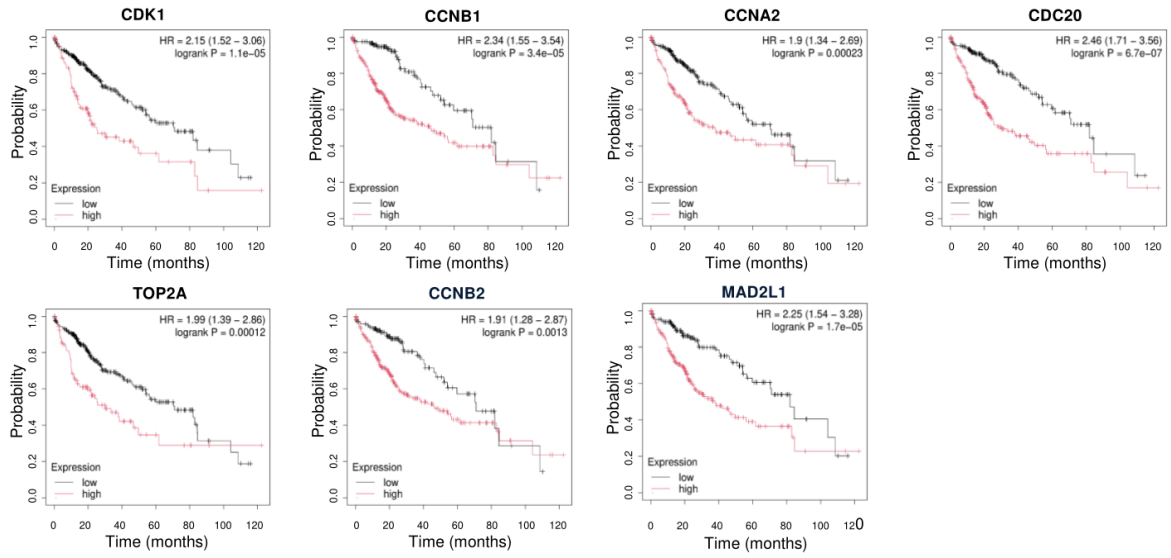

Figure 5. ***Survival analysis of potential hub genes in patients with liver cancer.***

IV. DISCUSSION

Hepatocellular carcinoma (HCC) is among the most aggressive malignancies, characterized by low survival rates largely due to diagnostic challenges and the limited effectiveness of current treatment options. In this context, identifying and validating novel therapeutic targets for HCC is an urgent priority to improve treatment outcomes and patient prognosis. Integrated bioinformatics offers powerful tools to uncover the underlying diagnostic and prognostic mechanisms of various diseases, including HCC. The findings of this study highlight the potential of bioinformatics as a valuable approach for identifying drug targets and advancing HCC therapy.

In this study, the GSE147888, GSE101685, and GSE62232 datasets were analyzed to identify differentially expressed genes (DEGs) between HCC tissues and their normal counterparts. A total of 538 DEGs were identified, including 227 upregulated and 331 downregulated genes. Protein–protein interaction (PPI) network analysis revealed 528 nodes and 2099 edges. Hub genes were subsequently identified using the NetworkAnalyzer and MCODE plugins in Cytoscape followed by validated with GEPIA, HPA and Kaplan Meier Plotter. Ultimately, seven hub genes-CDK1, CCNB1, CCNA2, CDC20, TOP2A, CCNB2, and MAD2L1-were selected for drug identification purposes.

Numerous studies have demonstrated that these newly identified hub genes can function as oncogenes or promising cancer biomarkers. For instance, Wu et al. reported that targeting CDK1 can enhance anti-HCC activity, offering a rational combination strategy to improve the clinical effectiveness of sorafenib [6]. Du et al. found that AURKA is highly expressed in HCC and is associated with poor prognosis [7]. Meng et al. demonstrated that TOP2A may serve as both a biomarker and a therapeutic target for HCC [8]. CCNB2 may act as a prognostic factor and cancer promoter through the CCNB2/PLK1 signaling pathway in HCC as studied by Li et al [9]. Furthermore, Xiong et al. identified UBE2C as a prognostic marker in HCC, with evidence that its inhibition could serve as a potential therapeutic approach [10]. Therefore, further studies are needed to confirm the effectiveness of these candidates in HCC. These findings underscore the importance of further investigating the seven hub genes-CDK1, CCNB1, CCNA2, CDC20, TOP2A, CCNB2, and MAD2L1-to validate their potential as therapeutic targets in HCC.

V. CONCLUSION

In this study, three GEO gene expression datasets were systematically analyzed to identify differentially expressed genes (DEGs) associated with hepatocellular carcinoma (HCC). A total of 227 upregulated and 331 downregulated DEGs were consistently detected across all datasets. A protein–protein interaction (PPI) network was constructed, and 11 candidate hub genes were identified through topological analysis and clustering. These genes were further validated using GEPIA, the Human Protein Atlas, and Kaplan–Meier Plotter. Ultimately, seven hub genes—CDK1, CCNB1, CCNA2, CDC20, TOP2A, CCNB2, and MAD2L1—were confirmed to have both transcriptional and translational significance and to be strongly associated with poor prognosis in HCC. These findings highlight promising molecular targets for future diagnostic and therapeutic strategies in liver cancer.

LIST OF ABBREVIATIONS

AURKA	Aurora kinase A
CCNA2	Cyclin A2
CCNB1	Cyclin B1
CCNB2	Cyclin B2
CDC20	Cell Division Cycle 20
CDK1	Cyclin-dependent kinase 1
DEGs	Differentially expressed genes
GEO	Gene Expression Omnibus
GEPIA	Gene Expression Profiling Interactive Analysis
HCC	Hepatocellular carcinoma
HPA	Human Protein Atlas
IARC	International Agency for Research on Cancer
IHC	Immunohistochemistry
MAD2L1	Mitotic Arrest Deficient Like 1
PPI	Protein-Protein Interaction
TOP2A	DNA topoisomerase IIα
UBE2C	Ubiquitin conjugating enzyme E2 C
WHO	The World Health Organization

FUNDING SOURCES

Not applicable.

CONFLICTS OF INTERESTS

There were no conflicts of interest in this study.

AVAILABILITY OF DATA AND MATERIAL

Upon reasonable request, the datasets of this study can be available from the corresponding author.

REFERENCES

1. **Sung H, Ferlay J, Siegel RL, Laversanne M, Soerjomataram I, Jemal A, et al.** Global cancer statistics 2020: GLOBOCAN estimates of incidence and mortality worldwide for 36 cancers in 185 countries. CA: a cancer journal for clinicians. 2021;71(3):209-49.
2. **Liu J, Zhou S, Li S, Jiang Y, Wan Y, Ma X, et al.** Eleven genes associated with progression and prognosis of endometrial cancer (EC) identified by comprehensive bioinformatics analysis. Cancer Cell International. 2019;19(1):1-17.
3. **Zhang X, Liu S, Cai Y, Changyong E, Sheng J.** Screening and validation of independent predictors of poor survival in pancreatic cancer. Pathology and Oncology Research. 2021:115.
4. **Yang W-X, Pan Y-Y, You C-G.** CDK1, CCNB1, CDC20, BUB1, MAD2L1, MCM3, BUB1B, MCM2, and RFC4 may be potential therapeutic targets for hepatocellular carcinoma using integrated bioinformatic analysis. BioMed research international. 2019;2019.
5. **Regan-Fendt K, Li D, Reyes R, Yu L, Wani NA, Hu P, et al.** Transcriptomics-based drug repurposing approach identifies novel drugs against sorafenib-resistant hepatocellular carcinoma. Cancers. 2020;12(10):2730.
6. **Wu CX, Wang XQ, Chok SH, Man K, Tsang SHY, Chan ACY, et al.** Blocking CDK1/PDK1/β-Catenin signaling by CDK1 inhibitor RO3306 increased the efficacy of sorafenib treatment by targeting cancer stem cells in a preclinical model of hepatocellular carcinoma. Theranostics. 2018;8(14):3737.
7. **Du R, Huang C, Liu K, Li X, Dong Z.** Targeting AURKA in Cancer: molecular mechanisms and opportunities for Cancer therapy. Molecular cancer. 2021;20:1-27.
8. **Meng J, Wei Y, Deng Q, Li L, Li X.** Study on the expression of TOP2A in hepatocellular carcinoma and its relationship with patient prognosis. Cancer Cell International. 2022;22(1):1-18.
9. **Li R, Jiang X, Zhang Y, Wang S, Chen X, Yu X, et al.** Cyclin B2 overexpression in human hepatocellular carcinoma is associated with poor prognosis. Archives of medical research. 2019;50(1):10-7.
10. **Xiong Y, Lu J, Fang Q, Lu Y, Xie C, Wu H, et al.** UBE2C functions as a potential oncogene by enhancing cell proliferation, migration, invasion, and drug resistance in hepatocellular carcinoma cells. Bioscience reports. 2019;39(4).